Published in final edited form as:
Bioorg Med Chem. 2013 November 1; 21(21): . doi:10.1016/j.bmc.2013.08.042.

Binding Mode Characterization of 6α- and 6β-*N*-Heterocyclic Substituted Naltrexamine Derivatives via Docking in Opioid Receptor Crystal Structures and Site-directed Mutagenesis Studies: Application of the "Message–Address" Concept in Development of Mu Opioid Receptor Selective Antagonists

Saheem A. Zaidi[a], **Christopher K. Arnatt**[a], **Hengjun He**[b], **Dana E. Selley**[b], **Philip D. Mosier**[a], **Glen E. Kellogg**[a], and **Yan Zhang**[a]

Yan Zhang: yzhang2@vcu.edu

[a]Department of Medicinal Chemistry, Virginia Commonwealth University, Richmond, VA 23298, USA

[b]Department of Pharmacology and Toxicology, Virginia Commonwealth University, Richmond, VA 23298, USA

Abstract

Highly selective opioid receptor antagonists are essential pharmacological probes in opioid receptor structural characterization and opioid agonist functional studies. Currently, there is no highly selective, non-peptidyl and reversible mu opioid receptor antagonist available. Among a series of naltrexamine derivatives that have been designed and synthesized, two compounds, NAP and NAQ, were previously identified as novel leads for this purpose based on their *in vitro* and *in vivo* pharmacological profiles. Both compounds displayed high binding affinity and selectivity to the mu opioid receptor. To further study the interaction of these two ligands with the three opioid receptors, the recently released opioid receptor crystal structures were employed in docking studies to further test our original hypothesis that the ligands recognize a unique "address" domain in the mu opioid receptor involving Trp318 that facilitates their selectivity. These modeling results were supported by site-directed mutagenesis studies on the mu opioid receptor, where the mutants Y210A and W318A confirmed the role of the latter in binding. Such work not only enriched the "message-address" concept, also facilitated our next generation ligand design and development.

Keywords

Mu opioid receptor; selective antagonists; crystal structures; automated docking; site-directed mutagenesis; GPCR

Correspondence to: Yan Zhang, yzhang2@vcu.edu.

Supporting Information Available: GOLD docking summary: the top ten scores from the last trial in the automatic docking for all four ligands. This material is available free of charge via the Internet at http://pubs.acs.org.

Introduction

Because receptor-selective opioid antagonists are vital tools for identifying the receptor types involved in interactions with selective opioid agonists, such antagonists have played very important roles in the study of opioid receptors. In general, an agonist interaction is characterized as opioid receptor-mediated only if its effect is competitively inhibited by an opioid antagonist.[1–3] More specifically, characterization of the mu opioid receptor (MOR) structure–function relationship is essential because the analgesic effect, addictive properties, and notorious side effects (such as addiction/abuse liability, respiratory depression, and constipation) of the key drug morphine are abolished in MOR knock-out mice, indicating that these side effects are primarily due to its interaction with the MOR.[4–6] Yet, the lack of a non-peptidyl, highly selective, reversible, and potent MOR antagonist limits our understanding of the structure–function relationship of the MOR, the interaction of nonpeptidyl MOR agonists with it, and more significantly, the activation mechanism of the receptor with respect to its role in drug abuse and addiction.

As one of the most serious chronic and relapsing medical disorders, heroin and prescription opioid abuse and dependence are very common, and still increasing.[7] Another serious substance addiction disease is alcoholism. It is reported that disorders related to alcohol abuse affect 7–8% of Americans at any given time, or about 15 to 20 million adults, while these disorders account for $185 billion in U.S. health care costs, lost wages, bodily injury, and property damage annually.[8–9] Some antagonists with relatively low selectivity for the MOR, e.g., naltrexone and naloxone, have been shown to be able to block relapse and curb drug craving in opiate addicts as well as to treat alcoholism.[10–15] Although these antagonists have shown promise in these treatments, some severe side effects have been reported, likely due to their lack of selectivity. For example, patients receiving naltrexone for opioid dependence exhibited higher than expected rates of overdose and suicide, and some reports have linked this drug with depression and dysphoria.[16–18] Evidence has accumulated that the delta opioid receptor (DOR) may be connected to mood-related behavior,[19–21] while the kappa opioid receptor (KOR) may play an important role in the inhibition of glycinergic neurotransmission to cardiac vagal neurons.[22] Therefore, a new antagonist with drug-like properties and high selectivity for the MOR may be a very promising medication for treatment of drug addiction and alcoholism.

Based on the “message–address concept”,[23,24] highly selective non-peptide antagonists for the KOR (e.g., norBNI and GNTI)[25,26] and for the DOR (e.g., NTI)[27] were designed and synthesized more than two decades ago. These compounds are widely used as selective ligands in pharmacological studies. Thus far, however, no optimal antagonist has been developed for the MOR, though some moderately potent ligands, e.g., cyprodime,[28] are in use. Compared with the high selectivity of GNTI[26] for the KOR (K_i ratios: MOR/KOR≈120, DOR/KOR≈250) and NTI[27] for the DOR (K_i ratios: MOR/DOR≈152, KOR/DOR≈276), cyprodime[29] has only moderate selectivity for the MOR (K_i ratios: KOR/MOR≈45, DOR/MOR≈40). Another drawback of cyprodime is that it shows much lower affinity for the MOR than naloxone and naltrexone, which limits its application. Also, while selective, but irreversible, antagonists for the MOR such as β-FNA, clocinnamox and others have been reported,[30–31] their potential covalent binding with the receptor limits their utility: reversible antagonists are usually preferred because they can temporarily “knock out” receptors for pharmacological studies, and then be washed out from the binding locus to “revive” the receptors.

Most of the highly selective and reversible MOR antagonists currently available are conformationally constrained peptides, e.g., D-Phe-Cys-Tyr-D-Trp-Orn-Thr-Pen-Thr-NH_2 (CTOP) and D-Phe-Cys-Tyr-D-Trp-Arg-Thr-Pen-Thr-NH_2 (CTAP). They are relatively stable

metabolically and have been used to target the MOR with *in vitro* and *in vivo* studies.[32] However, their limited bioavailability, i.e., relatively poor ability to cross the blood–brain barrier, render them not generally suitable for many types of *in vivo* studies and certainly not suitable for medical applications.[33,34] The utility of an antagonist as a pharmacological tool is significantly enhanced if it has both *in vitro* and *in vivo* activity; thus, non-peptide ligands are preferred for their better ability to penetrate the CNS and for their lesser vulnerability to metabolic inactivation. Therefore, the development of a non-peptide, potent, selective and reversible antagonist for the MOR remains highly desirable.

We recently reported a series of novel ligands that were designed based on our homology modeling of the three opioid receptor subtypes.[35] They were experimentally characterized as MOR selective antagonists in the in vitro and in vivo studies. In particular, two compounds (NAP and NAQ; Figure 1) showed predominant binding affinity to the MOR over both the DOR and the KOR, and possessed only marginal agonist efficacy at the MOR in the radioligand binding assays. In calcium flux functional assays, either ligand showed any significant agonist activity compared to the MOR full agonist DAMGO while in the DAMGO agonism inhibitory activity studies, NAP showed IC_{50} at 19.5 ± 5.5 nM and NAQ at 150 ± 9.4 nM. Such results were in line with their radioligand binding affinity though at a relatively lower level. Therefore, these two compounds are defined as our leads for further development of non-peptidyl MOR antagonists. For the next stage of molecular design, an understanding of the interaction of these two leads with the opioid receptors and the resulting MOR selectivity at an atomic level is critical. The many recent depositions of high-resolution GPCR crystal structures, including opsin, the human β_2- and β_1-adrenergic receptors, the human A_{2A} adenosine receptor, chemokine receptor CXCR4, dopamine D3 receptor, sphingosine 1-phosphate receptor 1 and histamine receptor H1, among others,[36] has transformed structure-based drug discovery for GPCR targets. The release of three opioid receptor subtype (MOR, KOR and DOR) crystal structures[37–39] last year was one of the most exciting breakthroughs in opioid receptor research field in decades. Here, we report docking studies of NAP and NAQ into these three experimental structures, combined with primary site-directed mutagenesis studies that validate the modeling observations. These results facilitate our understanding of the receptor–ligand interactions involved in the observed MOR selectivity and will inform our future work.

Results and Discussion

Sequence alignment analyses of three opioid receptors

In our original efforts to conduct structure-based design of novel ligands as selective MOR antagonists, we adopted homology modeling methods simply because there were no x-ray crystal structures for any of the opioid receptors, and in fact, any G-protein coupled receptors (GPCR) other than bovine rhodopsin. Analysis of sequence alignments of all three opioid receptors along with bovine rhodopsin (Figure 2) not only provided us the three dimensional conformation motif, but also revealed that: 1) the three human opioid receptors share very high homology (over 60% sequence identity); 2) a generally higher sequence identity is observed for the ligand binding pockets believed to be formed primarily by transmembrane (TM) helices 2, 3, 6 and 7 (the so-called “message” domain of the receptor), and this is in line with the similar structural features of many opioid receptor ligands (Figure 1) representing the “message” moiety of these ligands; 3) an even higher identity (close to 90%) is seen for the intracellular loop (ICL) regions, which is because the three opioid receptors share the same family of G-proteins ($G_{i/o}$) for signal transduction, and the G-protein binding domain of the receptor is mainly on the ICL loci; and 4) much lower sequence identities were observed in the extracellular loop (ECL) regions, and for both N- and C termini. More strikingly, ECL3 of the three opioid receptors carried the lowest sequence identity of all domains (Table 1). The location of ECL3 directly above the

"message" region of the binding site helped us to define a potential "address" domain in the MOR, which we used in designing our MOR-selective antagonists.[35] Our ability, now, to compare the three opioid receptor crystal structures by domain gives us nearly identical results, which is further validation for our original molecular design strategy.

Small molecule construction and conformational analysis

Models for the small molecules NAP, NAQ and naltrexone (NTX) were built prior to conformational analysis of the first two. Then, brief dynamics simulations were conducted for NAP and NAQ within a periodic water box. Due to the partial double bond in the amide linkage of the two compounds, they adopted either an "*anti*" or "*syn*" conformation, as shown for NAP (Figure 3). The averaged conformations measured from the last 10 ns of dynamics (of the total 100 ns) for both ligands were predominantly *anti*, which is expected to be more thermodynamically favorable of the two conformations.

Docking studies of the opioid universal antagonist NTX

Previously, we used NTX as a probe to propose the "address" binding domain within the MOR antagonist binding pocket with homology-derived models of the three opioid receptors.[35] Similar regions have been implicated as the binding loci for various peptide and non-peptide ligands.[40–42] In the present study, NTX was docked in a similar fashion within a pocket formed by helices 3, 6 and 7 in each receptor X-ray crystal structure using the GOLD[43] docking program. The conformations of the ligands co-crystallized in the receptors were used as starting points for docking. In this way, the docking problem was transformed into the much simpler issue of energetically placing just the 6-position side chain NTX, as there is a common core for it and the ligands bound in the crystal structures; β-funaltrexamine in the MOR, naltrindole in the DOR and JDTic in the KOR (see Figure 1). This guided docking of NTX was followed by energy minimization to optimize the structural models for the ligand–receptor complexes. Two scoring systems were used to quantitatively characterize the binding poses. The CHEM-PLP score, the default scoring function of GOLD, which has been optimized for modeling steric complementarity between ligand and protein along with distance- and angle-dependent hydrogen bonding, was used to obtain plausible docking poses. The obtained poses were then rescored with HINT (Hydropathic INTeractions), an empirical free energy scoring tool based on the experimental measurements of logP for 1-octanol and water,[44] to estimate atomic level free energies associated with non-covalent interactions.[45,46] Optimal docking poses for each NTX–receptor complex were chosen by the highest CHEM-PLP and HINT scores, which were, in this case, generally in agreement (Table 3).

Amino acid residues shown to interact with the ligand were highly conserved among the three opioid receptors (Figure 4). Asp$^{3.32}$ was involved in an ionic interaction with the 17-position tertiary amino group of the ligand while Tyr$^{3.33}$ formed a hydrogen bond with the dihydrofuranyl oxygen (superscripts "x.yy" refer to Ballesteros–Weinstein numbering[48]). The orientation of the 3-phenolic hydroxyl group also indicated the likelihood of a hydrogen bonding interaction with His$^{6.52}$ through two water molecules, as seen in MOR and KOR crystal structures. Lys$^{5.39}$ may be involved in hydrogen bonding interactions with the 6-position carbonyl oxygen atom and Met$^{3.36}$, Trp$^{6.48}$, Ile$^{6.51}$, Val/Ile$^{6.55}$, Ile$^{7.39}$ and Tyr$^{7.43}$ formed a hydrophobic pocket to accommodate the morphinan skeleton of the molecule.

Docking studies of NAP and NAQ

Among a series of novel ligands designed and synthesized to target the "address" domain of the MOR, NAP and NAQ have sub-nanomolar affinity for the MOR and high selectivity over the DOR and the KOR from *in vitro* radioligand competition binding studies. Both showed only marginal partial agonism in the *in vitro* GTPγS assay and potent antagonism in

an *in vivo* antinociceptive test against morphine.[35] Our initial molecular modeling study suggested that the MOR selectivity for these two ligands could be the result of the previously identified hydrogen bonding between the ligand and the MOR "address" binding locus.[35] To further understand how these two lead compounds can have similar affinities and selectivities for the MOR, despite significant chemical differences in their side chain structures, we revisited our docking study by employing the x-ray crystal structure models for the opioid receptors, again using GOLD,[45] and the conformations of the co-crystallized ligands as starting points. As with NTX, there is a common core for our ligands and those in the three crystal structures. This was followed by energy minimization of the NAP and NAQ ligand receptor complex models. The results of the docking experiments are presented in Figures 5, 6 and 7.

Analysis of the NAP and NAQ morphinan backbone binding site

As noted above, all three opioid receptors share a very high degree of sequence similarity in the "message" region of ligand-binding pocket. As a result, the morphinan nucleus of NAP and NAQ were both found to be docked within each receptor in a similar fashion as NTX. The composition of the binding pockets is, in fact, practically identical. In other words, the "message" component of the ligands occupied the "message" domain in the receptor. On the other hand, docking results showed that the side chains of the ligands, i.e., the "address" component of the ligands, primarily clustered around two different binding sites in the three opioid receptors: Site 1 located at the top of helix 6 and 7 (including part of ELC3) and Site 2 at the top of helix 5 and ECL2 (see Figures 5–7).

NAP and NAQ in the MOR

Clustering of the docked poses for NAP in the MOR revealed two high scoring pose families related to the two "address" sites suggested above (see Table 3). For one pose, NAP adopted a "*syn*" conformation at the amide linkage with the pyridinyl substituent pointing towards Site 1, where the side chain could stack with Trp318$^{7.35}$ with π-π interactions in addition to a possible hydrogen bond (Figure 5A). Also, Lys303$^{6.58}$ may form a hydrogen bond with the pyridinyl nitrogen of NAP. For the second pose, the ligand indicated its amide linkage to be in the "*anti*" conformation with the pyridinyl side chain placed in a hydrophobic pocket (Site 2) at the top of helix 5 and near ECL2 (Figure 5B). However, the presence of Glu229$^{5.35}$, which is close to the pyridinyl side chain, led to a highly negative (i.e. unfavorable) interaction that is reflected by the lower HINT score for this pose (Table 3). Thus, it is likely that NAP prefers interaction with Site 1. NAQ followed a similar pattern in its docking solutions, except that, in both binding sites, the ligand adopted the "*syn*" conformation. As with NAP in Site 1, the quinolinyl side chain of NAQ appears to interact with Trp318$^{7.35}$ with π-π stacking, while in Site 2 (Figure 5C), the side chain has an unfavorable interaction with Glu229$^{5.35}$ (Figure 5D). Meanwhile, Lys303$^{6.58}$ may also possibly form a hydrogen bond in both binding sites, not with the quinolinyl nitrogen atom of NAQ, but with the spacer portion of the molecule.

NAP and NAQ in the KOR

As in the MOR, docking of NAP in the KOR gave two favorable binding poses. However, in both sites of the KOR, the ligand adopts only the "*anti*" conformation to achieve high docking scores. In Site 1, although the aromatic side chain may interact with Tyr312$^{7.35}$ with π-π interactions, the presence of Glu297$^{6.58}$ in place of Lys303$^{6.58}$ of the MOR appears to cause deleterious interactions with the ligand side chain (Figure 6A). In Site 2 of the KOR, the Asp223$^{5.35}$ is one carbon shorter compared to the analogous Glu229$^{5.35}$ of the MOR, which results in lessened unfavorable interactions with the NAP side chain (Figure 6B). Moreover, the presence of Tyr219$^{5.31}$ and Ser211 (ECL2) may result in more favorable hydrogen bonding interactions with the nitrogen atom of the side chain. Based on these

results, NAP likely adopts Site 2 in the KOR. In contrast, NAQ seems to prefer a "*syn*" conformation in both its KOR docking poses (Figures 6C, D). The larger hydrophobic group (quinolinyl side chain) of NAQ may result in even more significant hydropathic incompatibility with Glu297$^{6.58}$, probably negating the thermodynamically favorable aromatic π- stacking interactions of that side chain with Tyr312$^{7.35}$ at Site 1. Also, HINT scores for NAQ binding in Site 2 (Table 3) indicated no negative interactions with Asp223$^{5.35}$, while allowing for the possibility of hydrogen bonding between the side chain and Tyr219$^{5.31}$ and/or Ser211 (ECL2).

NAP and NAQ in the DOR

For docking NAP in the DOR, the ligand adopted a "*syn*" conformation in Site 1 with the side chain stacked in a hydrophobic pocket formed by Trp284$^{6.58}$ and Leu300$^{7.35}$ (Figure 7A), while in Site 2 it was in an "*anti*" conformation with the pyridinyl side chain placed in a hydrophobic pocket close to the top of helix 5 and ECL2 (Figure 7B). Notably, these putative interactions failed to utilize any of the hydrogen bonding observed in the MOR and the KOR models, which may offer a reason for the lower affinity of NAP for the DOR. NAQ, except for a tendency for the "*syn*" conformation, adopted nearly identical binding poses as NAP.

Site-directed Mutagenesis

The above results indicated that plausible hydrogen bonding and aromatic stacking interactions between the "address" portions of the two lead compounds and TM7 residues of the MOR may be responsible for their high binding affinity to the MOR vs. the DOR and KOR. In particular, the role of Trp318$^{7.35}$ seemed to be the most critical. This conclusion is in partial agreement with our earlier homology model-based docking studies for these receptors,[35] which suggested possible roles for both Trp318$^{7.35}$ and Tyr210 (ECL2) in imparting ligand selectivity by recognizing their "address" portion specifically. To further verify the roles of these two residues in the MOR receptor "address" domain for the MOR selectivity of the NAP and NAQ leads, we performed a site-directed mutagenesis study with a transient Chinese hamster ovary (CHO) cell line transfected with wild type and mutated MORs. In these studies, either Trp318$^{7.35}$ or Tyr210 in MOR was mutated to alanine, and NTX was used as a control. As shown in Table 4, the binding affinities of the NTX control were largely unaffected for either mutated receptor compared to their wild types, which supported the observation from our docking studies that the common "message" portion of the ligands recognized the "message" domain of the receptor to achieve their opioid receptor function. On the other hand, both NAP and NAQ bound to the Y210A mutant with affinities comparable to those of wild type MOR, while their affinities were dramatically decreased for the W318A mutant. These results are in agreement with the docking results described above that indicated the preference of the aromatic NAP and NAQ side chains to π-stack and hydrogen bond with Trp318$^{7.35}$ of the MOR in Site 1 over Tyr210 (ECL 2) in Site 2. The docking scores of NTX, NAP and NAQ in models of the mutant MOR structures were consistent with experimental results. Together, all of these observations validate our hypothesis that these two leads may recognize an alternative "address" locus in the MOR to confer their selectivity for the mu over the delta and the kappa opioid receptors.

Conclusions

Highly selective opioid receptor antagonists are essential pharmacological probes in opioid receptor structural characterization. We hypothesized that the two novel naltrexamine derivatives NAP and NAQ, previously identified as leads for development as MOR antagonists based on their *in vitro* and *in vivo* pharmacological profiles, which included high binding affinity and selectivity for the MOR over the DOR and the KOR, may recognize a

unique “address” domain in the MOR that facilitates their selectivity for the receptor. They, along with NTX, were docked in the recently released crystal structures of three antagonist-bound opioid receptors. The modeling results suggest how these novel naltrexamine derivatives may bind to the three opioid receptors to maintain morphinan-like “message” interactions, while their 6-position side chains act as the “address” moiety. This latter component interacts with amino acid residues that are non-conserved among the opioid receptors to confer their selectivity for one receptor over others. Furthermore, these studies also suggest that there may be at least two “address” sites in the receptors, and that the preference of naltrexamine derivatives for these sites depends on the type of opioid receptor. Further site-directed mutagenesis studies of the MOR support the model by proving the importance of Trp318$^{7.35}$ in the “address” domain. Application of the “message–address” concept, combined with molecular modeling, site-directed mutagenesis and targeted synthesis, indeed helped us in designing and developing more selective ligands for the mu opioid receptor with different pharmacological profiles more recently.[49] The same would be expected for other receptor selective ligands design and discovery in the future.

Materials and methods

Sequence analysis and model building

The sequences of human opioid and bovine rhodopsin receptors were obtained from Universal Protein Resource (UniProt) (Entry code: P35372 (MOR), P41145 (KOR), P41143 (DOR) and P02699 (Bovine rhodopsin receptor). The X-ray crystal structures for MOR (4DKL), KOR (4DJH) and DOR (4EJ4) were retrieved from PDB Data Bank at http://www.rcsb.org. Molecular models were built for each receptor in SYBYL-X 2.0; hydrogens were added, Gasteiger–Hückel charges were assigned, and their positions were optimized while holding all heavy atoms fixed as an aggregate with the Tripos force field (TAFF).

Docking studies

Within SYBYL-X 2.0, the chemical structures of the two lead MOR ligands (NAP and NAQ) and the universal ligand NTX were sketched, and their Gasteiger–Hückel charges were assigned before energy minimization (10,000 iterations) with the TAFF. The genetic algorithm docking program GOLD 5.1 was used to perform the docking studies with standard default settings unless otherwise specified. The binding site was defined to include all atoms within 10 Å of the γ-carbon atom of Asp$^{3.32}$ for the three opioid crystal structures. Automated docking was performed with a distance constraint of 4 Å between the piperidine nitrogen of the ligands’ morphinan nucleus and Asp$^{3.32}$, and between the ligands’ dihydrofuran oxygen and the phenolic oxygen of Tyr$^{3.33}$. Based on the fitness scores and the binding orientation of each ligand within the binding cavity, the best GOLD-docked solution was selected and merged into the receptor. The combined receptor–ligand structures were energy-minimized using the parameters described above in order to remove clashes and minimize strain energy, thus optimizing the interactions between ligand and receptor within the binding pocket. These models were then optimized as previously described[45,46,47] and subjected to hydropathic analysis with the HINT program.[44]

Conformational analysis

The NAP and NAQ structures were solvated with a water box. The water box including the ligand was again minimized under conditions similar to those described above. Next, an NVT molecular dynamics simulation was performed in SYBYL-X 2.0 for 100 ns with periodic boundary conditions with a 2 fs time-step. The energy-minimized average for the last 10 ns of the simulation for both ligands is shown.

Site-directed mutagenesis

Single point mutations were introduced into the MOR cDNA, expressed in pcDNA3.1, by mutant strand synthesis reactions through thermal cycling (QuikChange™ Site-Directed Mutagenesis Kit, Stratagene). The mutation was confirmed by DNA sequencing, performed by the DNA Core facility at VCU. The resulting mutant cDNA constructs (in pcDNA 3.1) were transfected into CHO-K1 cells using Lipofectamine. After 48 h, transient transfected cells were harvested and membranes prepared. Receptor expression levels were first determined by [^{3}H]naloxone saturation binding analysis (i.e., with varying concentrations of [^{3}H]naloxone) to determine B_{max} values. Cells transfected with the wild-type MOR were adopted as a control. Competition binding assays were conducted following the previously described protocol.[35]

MOR calcium inhibition assays

MOR-CHO cells were transfected with Gqi5 pcDNA1 using Lipofectamine 2000 (Invitrogen) according to the manufacturer's recommended procedure and maintained in RPMI 1640 supplemented with 10% fetal bovine serum, 100 u/mL penicillin, 100 μg/mL streptomycin, and 1 mg/mL G418 at 37°C and 5% CO_2. 48 hours after transfection a total of 2,500,000 cells were spun down and brought back up in 8 mL of 50:1 HBSS:HEPES assay buffer. Cells were then plated at 25,000 cells per well into a clear bottom, black 96-well plate (Greiner Bio-one) and 50 μL of Fluo4 loading buffer (40 μL 2 μM Fluo4-AM (Invitrogen), 100 μL 2.5 mM probenacid, in 5 mL assay buffer) was added to bring the volume up to 130 μL. After incubating for 45 minutes, 50 μL of varying concentrations of ligands and controls were added and the plate was incubated for an additional 15 minutes. Plates were then read on a FlexStation3 microplate reader (Molecular Devices) at 494/516 ex/em for a total of 120 seconds. After 16 seconds of reading, 20 μL of 100 nM DAMGO (NIDA) in assay buffer, or assay buffer alone, was added to the wells to bring the total volume up to 200 μL. The changes in Ca^{2+} mobilization were monitored and peak height values were obtained using SoftMaxPro software (Molecular Devices). Nonlinear regression curves and IC_{50}'s were generated using GraphPad Prism. All experiments were repeated a total of three times.

Supplementary Material

Refer to Web version on PubMed Central for supplementary material.

Acknowledgments

The work was partially supported by PHS grant DA024022 (Y. Z.) and DA017204 (P. D. M.). The content in this work is solely the responsibility of the authors and does not necessarily represent the official views of the National Institute on Drug Abuse or the National Institutes of Health.

References

1. Zimmerman DM, Leander JD. Selective opioid receptor agonists and antagonists: research tools and potential therapeutic agents. J. Med. Chem. 1990; 33:895–902. [PubMed: 2155322]
2. Schmidhammer H. Opioid Receptor Antagonists. Prog. Med. Chem. 1998; 35:83–132. [PubMed: 10795400]
3. Eguchi M. Recent advances in selective opioid receptor agonists and antagonists. Med. Res. Rev. 2004; 24:182–212. [PubMed: 14705168]
4. Matthes HW, Maldonado R, Simonin F, Valverde O, Slowe S, Kitchen I, Befort K, Dierich A, Le Meur M, Dollé P, Tzavara E, Hanoune J, Roques BP, Kieffer BL. Loss of morphine-induced analgesia, reward effect and withdrawal symptoms in mice lacking the mu-opioid-receptor gene. Nature. 1996; 383:819–823. [PubMed: 8893006]

5. Skoubis PD, Matthes HW, Walwyn WM, Kieffer BL, Maidment NT. Naloxone fails to produce conditioned place aversion in mu-opioid receptor knock-out mice. Neuroscience. 2001; 106:757–763. [PubMed: 11682161]
6. Gaveriaux-Ruff C, Kieffer BL. Opioid receptor genes inactivated in mice: the highlights. Neuropeptides. 2002; 36:62–71. [PubMed: 12359497]
7. Substance Abuse and Mental Health Services Administration. NSDUH series H-32. Rockville, MD: Office of Applied Studies; 2007. Results from the 2006 National Survey on Drug Use and Health: national findings. (DHHS publication no. SMA 07-4293.)
8. Global status report: alcohol policy. Geneva: World Health Organization; 2004.
9. Updating estimates of the economic costs of alcohol abuse in the United States: estimates, update methods, and data. Bethesda, MD: National Institute on Alcohol Abuse and Alcoholism; 2000.
10. Contet C, Kieffer BL, Befort K. Mu opioid receptor: a gateway to drug addiction. Curr. Opin. Neurobiol. 2004; 14:370–378. [PubMed: 15194118]
11. Gold MS, Dackis CA, Pottash AL, Sternbach HH, Annitto WJ, Martin D, Dackis MP. Naltrexone, opiate addiction, and endorphins. Med. Res. Rev. 1982; 2:211–246. [PubMed: 6289026]
12. Gonzalez JP, Brogden RN. Naltrexone. A review of its pharmacodynamic and pharmacokinetic properties and therapeutic efficacy in the management of opioid dependence. Drugs. 1988; 35:192–213. [PubMed: 2836152]
13. Soyka M, Roesner S. New pharmacological approaches for the treatment of alcoholism. Expert Opin. Pharmacother. 2006; 7:2341–2353. [PubMed: 17109610]
14. Oslin DW, Berrettini WH, O'Brien CP. Targeting treatments for alcohol dependence: the pharmacogenetics of naltrexone. Addict Biol. 2006; 11:397–403. [PubMed: 16961767]
15. Anton RF. Naltrexone for the management of alcohol dependence. N. Engl. J. Med. 2008; 359:715–721. [PubMed: 18703474]
16. Miotto K, McCann M, Basch J, Rawson R, Ling W. Naltrexone and dysphoria: fact or myth? Am. J. Addict. 2002; 11:151–160. [PubMed: 12028745]
17. Ritter AJ. Naltrexone in the treatment of heroin dependence: relationship with depression and risk of overdose. Aust. N. Z. J. Psychiatry. 2002; 36:224–228. [PubMed: 11982544]
18. Van Dorp EL, Yassen A, Dahan A. Naloxone treatment in opioid addiction: the risks and benefits. Expert Opin. Drug Saf. 2007; 6:125–132. [PubMed: 17367258]
19. Baamonde A, Daugé V, Ruiz-Gayo M, Fulga IG, Turcaud S, Fournié-Zaluski MC, Roques BP. Antidepressant-type effects of endogenous enkephalins protected by systemic RB 101 are mediated by opioid delta and dopamine D1 receptor stimulation. Eur. J. Pharmacol. 1992; 216:157–166. [PubMed: 1327810]
20. Tejedor-Real P, Micó JA, Smadja C, Maldonado R, Roques BP, Gilbert-Rahola J. Involvement of delta-opioid receptors in the effects induced by endogenous enkephalins on learned helplessness model. Eur. J. Pharmacol. 1998; 354:1–7. [PubMed: 9726624]
21. Filliol D, Ghozland S, Chluba J, Martin M, Matthes HW, Simonin F, Befort K, Gavériaux-Ruff C, Dierich A, LeMeur M, Valverde O, Maldonado R, Kieffer BL. Mice deficient for delta- and mu-opioid receptors exhibit opposing alterations of emotional responses. Nat. Genet. 2000; 25:195–200. [PubMed: 10835636]
22. Wang X, Dergacheva O, Griffioen KJ, Huang ZG, Evans C, Gold A, Bouairi E, Mendelowitz D. Action of kappa and Delta opioid agonists on premotor cardiac vagal neurons in the nucleus ambiguus. Neuroscience. 2004; 129:235–241. [PubMed: 15489045]
23. Schwyzer R. ACTH: a short introductory review. Ann. N. Y. Acad. Sci. 1977; 297:3–26. [PubMed: 211904]
24. Portoghese PS, Lipkowski AW, Takemori AE. Binaltorphimine and nor-bionaltorphimine, potent and selective kappa opioid receptor antagonists. Life Sci. 1987; 40:1287–1292. [PubMed: 2882399]
25. Jones RM, Hjorth SA, Schwartz TW, Portoghese PS. Mutational evidence for a common kappa antagonist binding pocket in the wild-type kappa and mutant mu[K303E] opioid receptors. J. Med. Chem. 1998; 41:4911–4914. [PubMed: 9836606]

26. Portoghese PS, Sultana M, Nagase H, Takemori AE. Application of the message-address concept in the design of highly potent and selective non-peptide delta opioid receptor antagonist. J. Med. Chem. 1988; 31:281–282. [PubMed: 2828619]
27. Schmidhammer H, Burkard WP, Eggstin-Aeppli L, Smith CFC. Synthesis and biological evaluation of 14-alkoxymorphinans. 2. (−)-N-(cyclopropymethyl)-4-14-dimethoxymorphinan-6-one, a selective mu opioid receptor antagonist. J. Med. Chem. 1989; 32:418–421. [PubMed: 2536439]
28. Marki A, Monory K, Otvos F, Toth G, Krassnig R, Schmidhammer H, Traynor JR, Roques BP, Maldonado R, Borsodi A. Mu-opioid receptor specific antagonist cyprodime: characterization by in vitro radioligand and [35S]GTPgammaS binding assays. Eur J Pharmacol. 1999; 383:209–214. [PubMed: 10585536]
29. Portoghese PS, Takemori AE. Affinity labels as probes for opioid receptor types and subtypes. NIDA Res. Monogr. 1986; 69:157–168. [PubMed: 3020413]
30. Burke TF, Woods JH, Lewis JW, Medzihradsky F. Irreversible opioid antagonist effects of clocinnamox on opioid analgesia and mu receptor binding in mice. J. Pharmacol. Exp. Ther. 1994; 271:715–721. [PubMed: 7965787]
31. Hawkins KN, Knapp RJ, Lui GK, Gulya K, Kazmierski W, Wan YP, Pelton JT, Hruby VJ, Yamamura HI. [3H]-[H-D-Phe-Cys-Tyr-D-Trp-Orn-Thr-Pen-Thr-NH2] ([3H]CTOP), a potent and highly selective peptide for mu opioid receptors in rat brain. J. Pharmacol. Exp. Ther. 1989; 248:73–80. [PubMed: 2563293]
32. Kramer TH, Shook JE, Kazmierski W, Ayres EA, Wire WS, Hruby VJ, Burks TF. Novel peptidic mu opioid antagonists: pharmacologic characterization in vitro and in vivo. J. Pharmacol. Exp. Ther. 1989; 249:544–551. [PubMed: 2566679]
33. Hruby VJ, Toth G, Gehrig CA, Kao LF, Knapp R, Lui GK, Yamamura HI, Kramer TH, Davis P, Burks TF. Topographically designed analogues of [D-Pen,D-Pen5]enkephalin. J. Med. Chem. 1991; 34:1823–1830. [PubMed: 1648137]
34. Abbruscato TJ, Thomas SA, Hruby VJ, Davis TP. Blood-brain barrier permeability and bioavailability of a highly potent and mu-selective opioid receptor antagonist, CTAP: comparison with morphine. J. Pharmacol. Exp. Ther. 1997; 280:402–409. [PubMed: 8996221]
35. Li G, Aschenbach LC, Chen J, Cassidy MP, Stevens DL, Gabra BH, Selley DE, Dewey WL, Westkaemper RB, Zhang Y. Design, synthesis, and biological evaluation of 6alpha- and 6beta-N-heterocyclic substituted naltrexamine derivatives as mu opioid receptor selective antagonists. J. Med. Chem. 2009; 52:1416–1427. [PubMed: 19199782]
36. Jacobson KA, Costanzi S. New Insights for Drug Design from the X-Ray Crystallographic Structures of G-Protein-Coupled Receptors. Mol. Pharmacol. 2012; 82:361–371. [PubMed: 22695719]
37. Manglik A, Kruse AC, Kobilka TS, Thian FS, Mathiesen JM, Sunahara RK, Pardo L, Weis WI, Kobilka BK, Granier S. Crystal structure of the μ-opioid receptor bound to a morphinan antagonist. Nature. 2012; 485:321–326. [PubMed: 22437502]
38. Wu H, Wacker D, Mileni M, Katritch V, Han GW, Vardy E, Liu W, Thompson AA, Huang XP, Carroll FI, Mascarella SW, Westkaemper RB, Mosier PD, Roth BL, Cherezov V, Stevens RC. Structure of the human κ-opioid receptor in complex with JDTic. Nature. 2012; 485:327–332. [PubMed: 22437504]
39. Granier S, Manglik A, Kruse AC, Kobilka TS, Thian FS, Weis WI, Kobilka BK. Structure of the δ-opioid receptor bound to naltrindole. Nature. 2012; 485:400–404. [PubMed: 22596164]
40. Seki T, Minami M, Nakagawa T, Ienaga Y, Morisada A, Satoh M. DAMGO recognizes four residues in the extracellular loop to discriminate between μ- and κ-opioid receptors. Eur. Jur. Pharmacol. 1998; 350:301–310.
41. Ulens C, Baker L, Ratka A, Waumans D, Tytgat J. Morphine-6beta-glucuronide and morphine-3-glucuronide, opioid receptor agonists with different potencies. Biochem. Pharmacol. 2001; 62:1273–1282. [PubMed: 11705461]
42. Xu H, Lu Y, Partilla JS, Zheng Q, Wang J, Brine GA, Carroll FI, Rice KC, Chen K, Chi Z, Rothman RB. Opioid peptide receptor studies, 11: involvement of Tyr148, Trp318 and His319 of

the rat mu-opioid receptor in binding of mu-selective ligands. Synapse. 1999; 32:23–28. [PubMed: 10188634]

43. Hartshorn MJ, Verdonk ML, Chessari G, Brewerton SC, Mooij WT, Mortenson PN, Murray CW. Diverse, high-quality test set for the validation of protein-ligand docking performance. J. Med. Chem. 2007; 50:726–741. [PubMed: 17300160]
44. Kellogg GE, Abraham DJ. Hydrophobicity: Is $LogP_{o/w}$ More than the Sum of its Parts? Eur. J. Med. Chem. 2000; 35:651–661. [PubMed: 10960181]
45. Spyrakis F, Amadasi A, Fornabaio M, Abraham DJ, Mozzarelli A, Kellogg GE, Cozzini P. The consequences of scoring docked ligand conformations using free energy correlations. Eur. J. Med. Chem. 2007; 42:921–933. [PubMed: 17346861]
46. Kellogg GE, Chen DL. The importance of being exhaustive. Optimization of bridging structural water molecules and water networks in models of biological systems. Chem. Biodivers. 2004; 1:98–105. [PubMed: 17191777]
47. Tripathi A, Fornabaio M, Kellogg GE, Gupton JT, Gewirtz DA, Yeudall WA, Vega NE, Mooberry SL. Docking and hydropathic scoring of polysubstituted pyrrole compounds with antitubulin activity. Biorg. Med. Chem. 2008; 16:2235–2242.
48. Ballesteros JA, Weinstein H. Integrated methods for the construction of three-dimensional models and computational probing of structure-function relations in G protein-coupled receptors. Methods Neurosci. 1995; 25:366–428.
49. Yuan Y, Elbegdorj O, Chen J, Akubathini SK, Zhang F, Stevens DL, Beletskaya IO, Scoggins KL, Selley DE, Akbarali HI, Dewey WL, Zhang Y. Design, Synthesis, and Biological Evaluation of 17-Cyclopropylmethyl-3,14β-dihydroxy-4,5α-epoxy-6β-[(4'-pyridyl)carboxamido]morphinan Derivatives as Peripheral Selective Mu Opioid Receptor Antagonists. J. Med. Chem. 2012; 55(22): 10118–10129. [PubMed: 23116124]

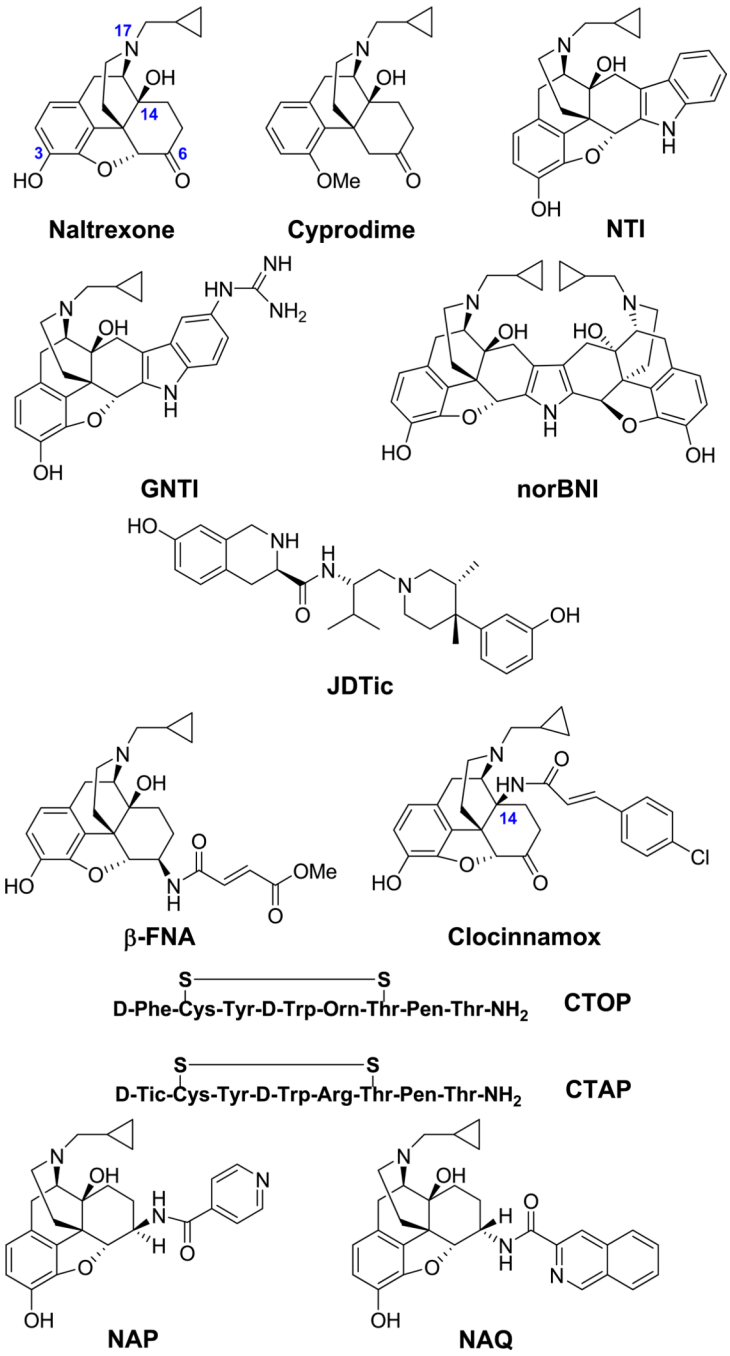

Figure 1.
Representative opioid receptor-selective antagonists.

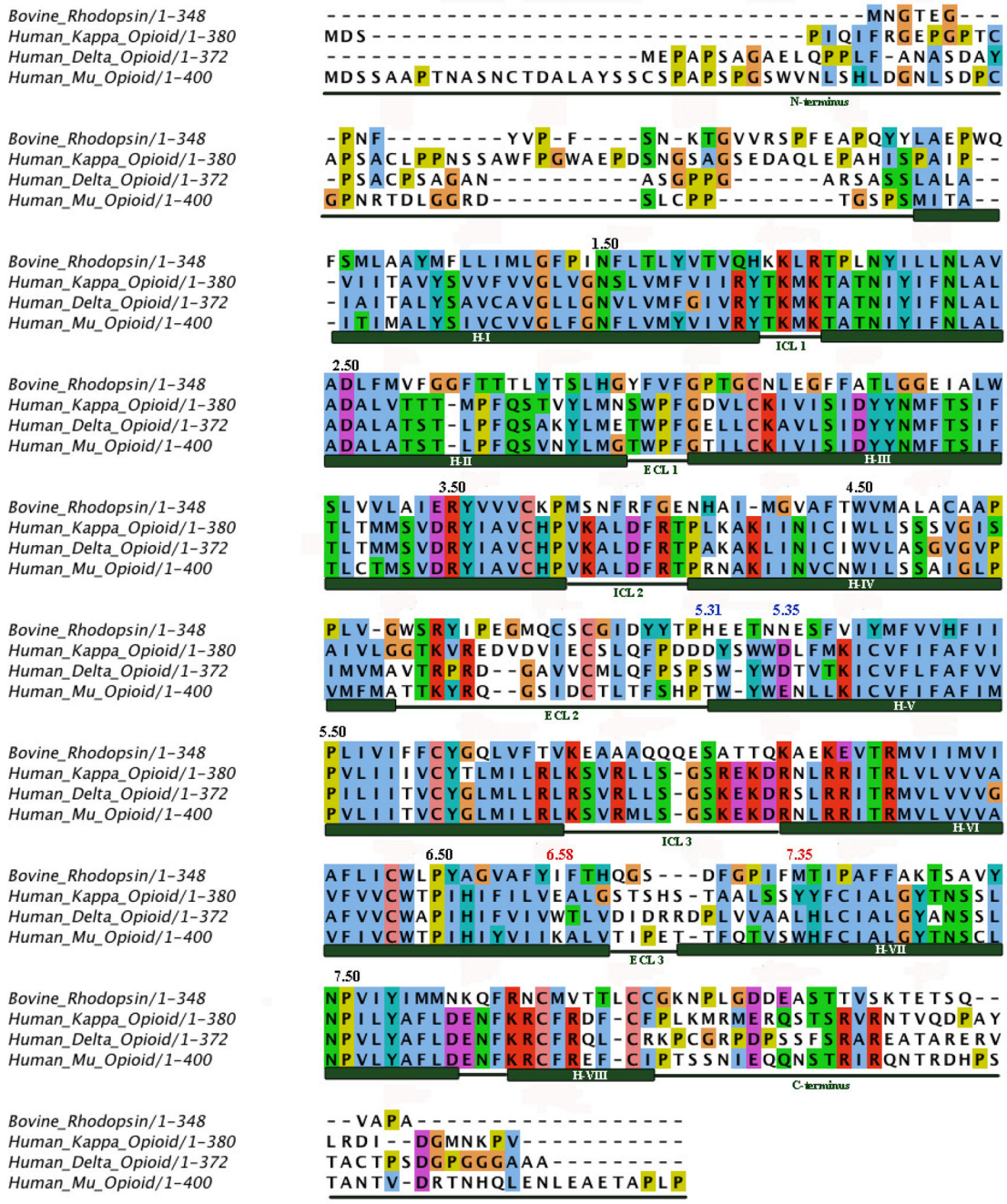

Figure 2.

Sequence alignment of opioid receptors and bovine rhodopsin. Ballesteros–Weinstein indices are indicated for the most conserved residues in each trans-membrane helix (black), important residues for Site 1 (red) and important residues for Site 2 (blue).

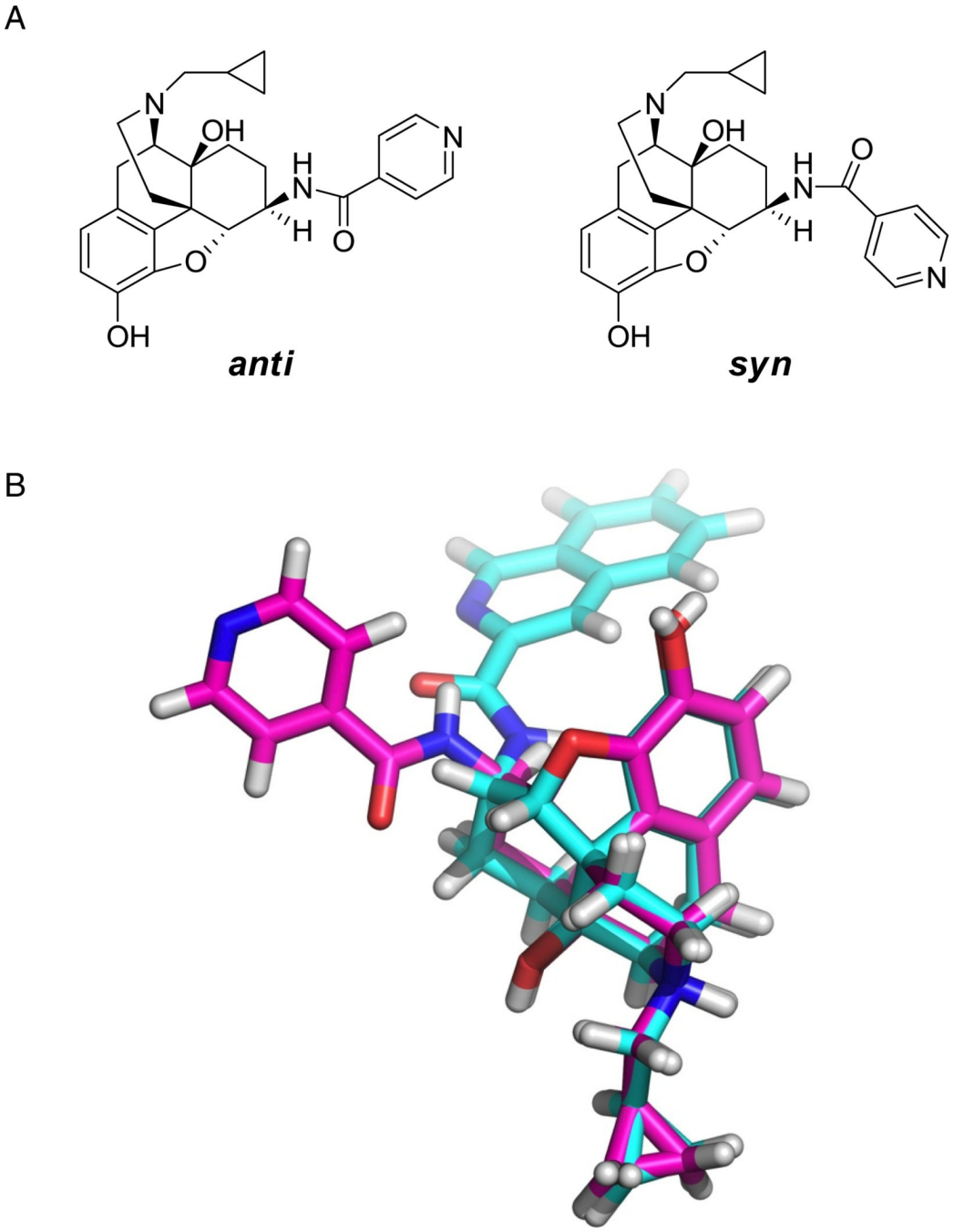

Figure 3.

A) Representation of "anti" and "*syn*" conformations for NAP. B) Conformational analysis results for NAP (magenta) and NAQ (cyan). Superimposed average structure for last 10 ns of a 100 ns NVT dynamic simulation inside a water box with PBC. Both NAP and NAQ preferred "anti" conformation over "*syn*".

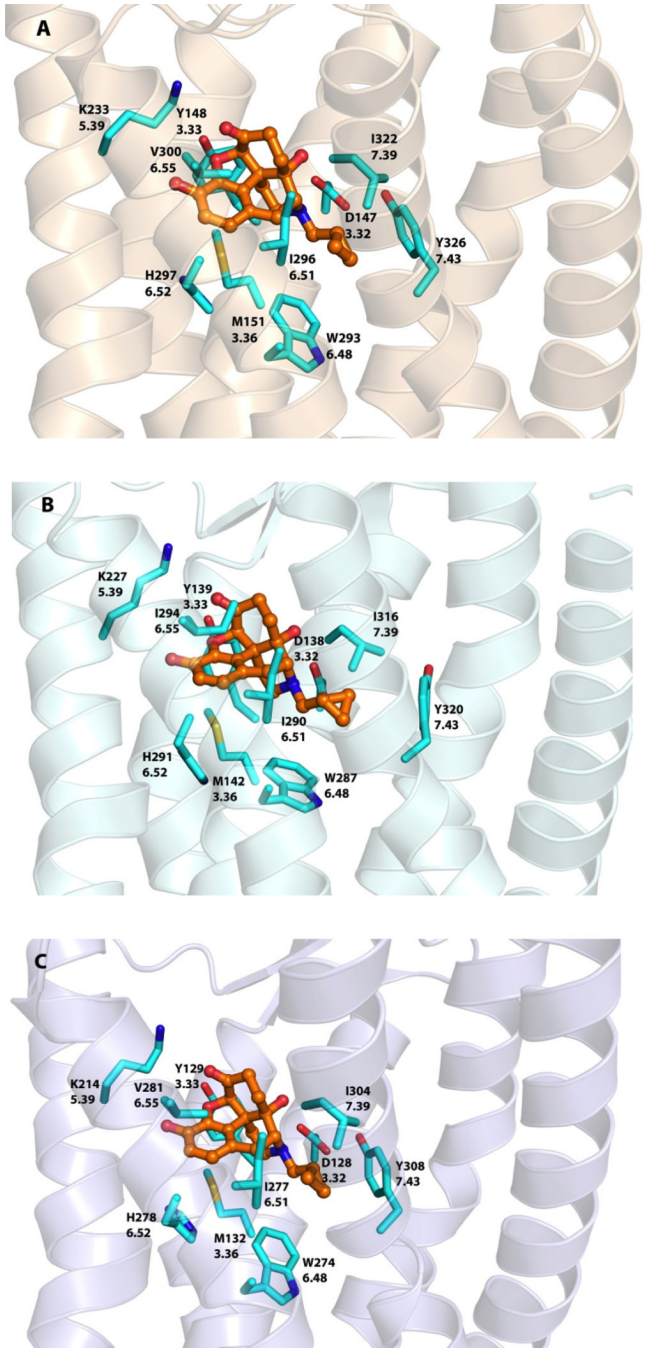

Figure 4.

Docked poses of NTX (orange carbon atoms) inside three opioid receptor crystal structures: A) MOR B) KOR and C) DOR. Amino acid residue atoms: carbon (cyan), oxygen (red), nitrogen (blue), sulfur (yellow).

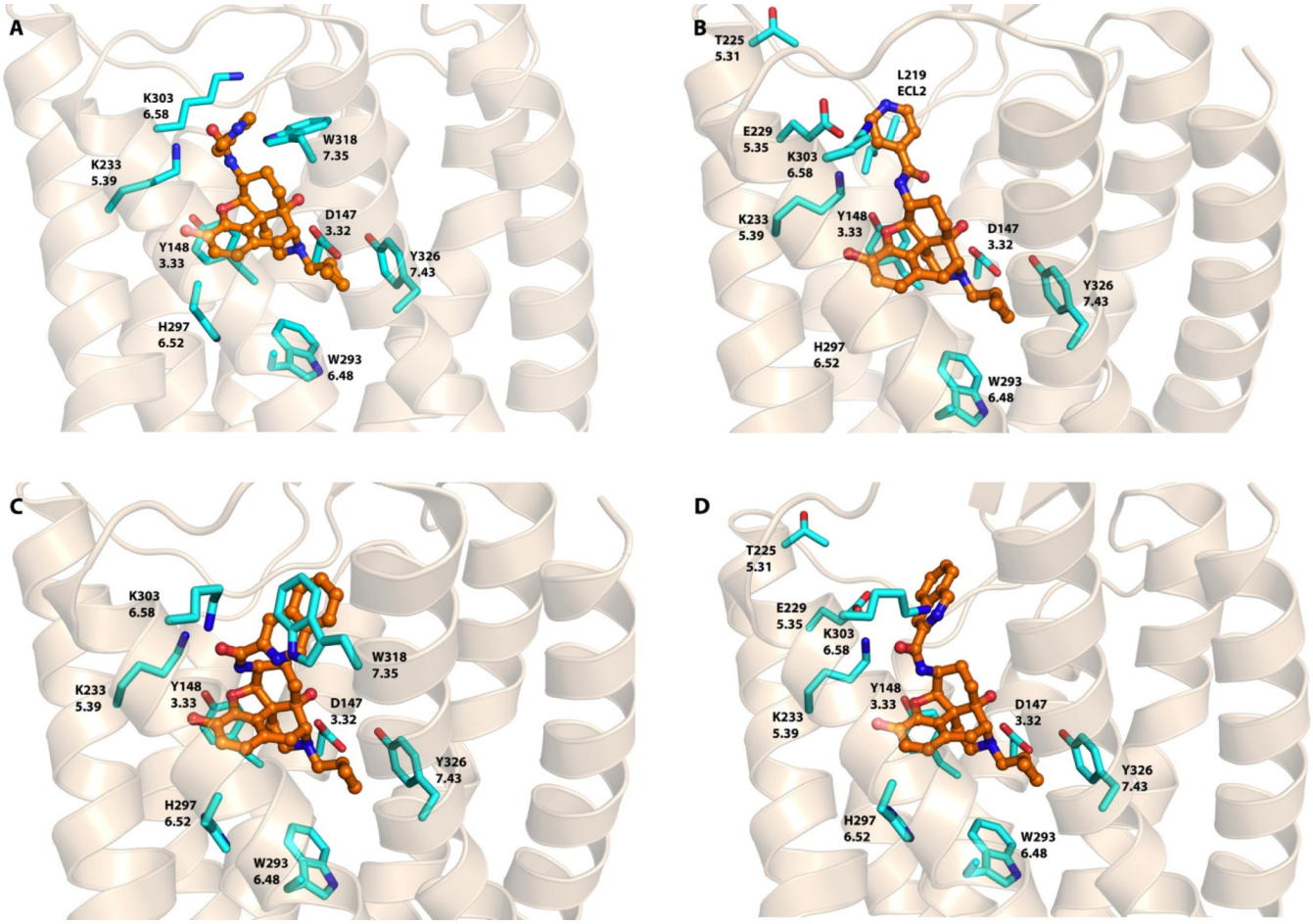

Figure 5.

Docked poses of NAP and NAQ in the mu opioid receptor. A) NAP in MOR binding Site 1. B) NAP in MOR binding Site 2. C) NAQ in MOR binding Site 1. D) NAQ in MOR binding Site 2. NAP and NAQ atoms: carbon (orange); amino acid residue atoms carbon: (cyan), oxygen (red), nitrogen (blue), sulfur (yellow).

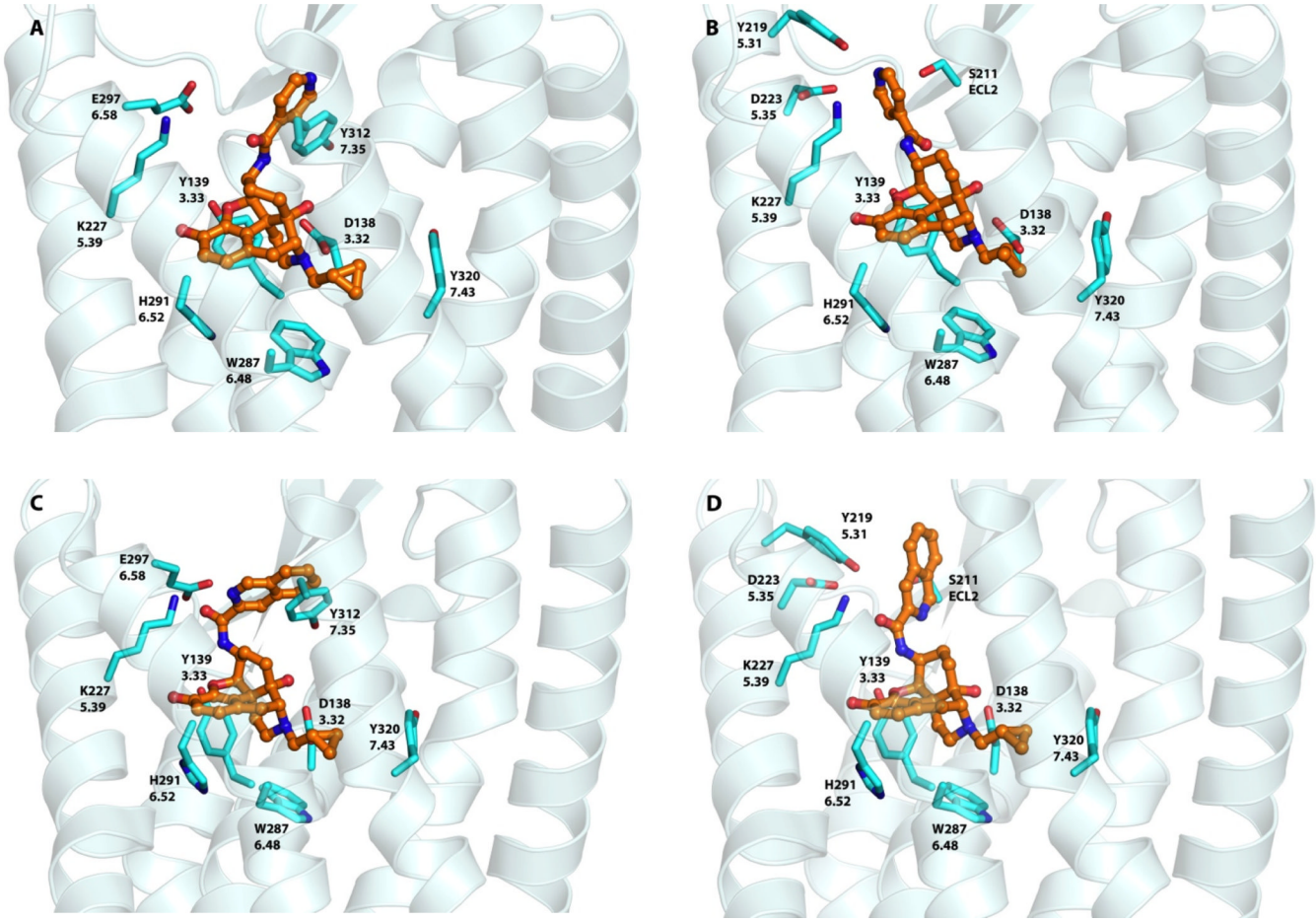

Figure 6.

Docked poses of NAP and NAQ in the kappa opioid receptor. A) NAP in KOR binding Site 1. B) NAP in KOR binding Site 2. C) NAQ in KOR binding Site 1. D) NAQ in KOR binding Site 2.

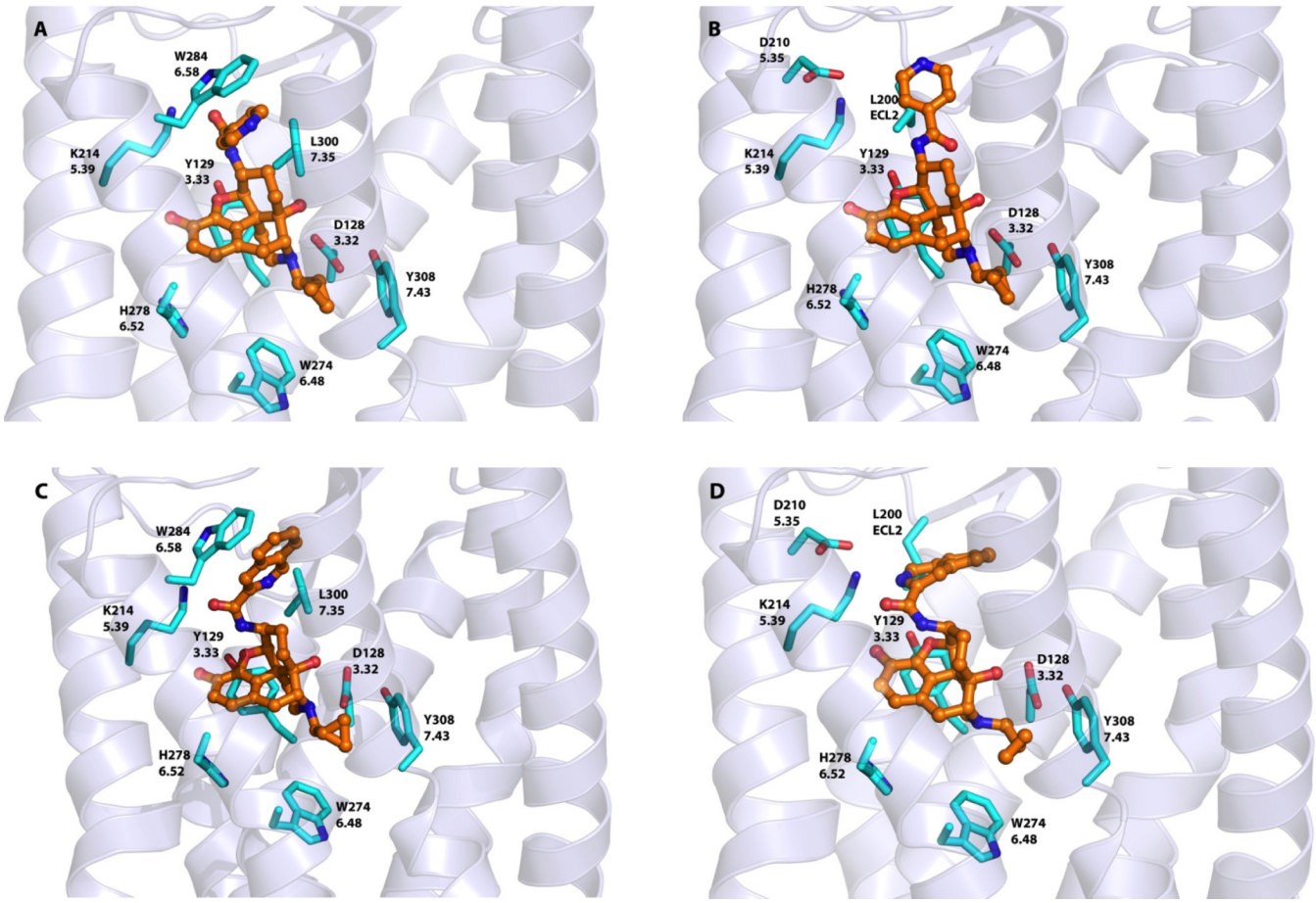

Figure 7.
Docked poses of NAP and NAQ in the delta opioid receptor. A) NAP in DOR binding Site 1. B) NAP in DOR binding Site 2. C) NAQ in DOR binding Site 1. D) NAQ in DOR binding Site 2.

Table 1

Comparison of the amino acid sequence identity among opioid receptors by domain.

	Percent sequence identity		
Domain	**Delta/mu**	**Delta/kappa**	**Mu/kappa**
TM1	69	62	62
TM2	95	86	82
TM3	90	95	100
TM4	43	57	33
TM5	85	77	77
TM6	73	64	73
TM7	78	82	86
EL1	73	67	67
EL2	52	52	30
EL3	**21**	**13**	**21**
IL1	90	90	100
IL2	91	95	91
IL3	86	81	86
N-terminus	28	33	18
C-terminus	40	32	35
Entire protein	62	61	57

Table 2

The non-conserved amino acid residue composition of the two binding sites in the three opioid receptors.

Receptor	Site 1	Site 2
MOR	$K303^{6.58}$ and $W318^{7.35}$	$E229^{5.35}$ and $T225^{5.31}$
KOR	$E297^{6.58}$ and $Y312^{7.35}$	$D223^{5.35}$ and $Y219^{5.31}$
DOR	$W284^{6.58}$ and $L300^{7.35}$	$D210^{5.35}$ and $S206^{5.31}$

Table 3

The GOLD (CHEM-PLP) and HINT scores for the best binding poses in the three opioid receptors.

Compounds	Docking pose[a]	MOR		KOR		DOR	
		CHEM-PLP	HINT[b]	CHEM-PLP	HINT[b]	CHEM-PLP	HINT[b]
NTX		79	1140	69	1009	85	1035
NAP	Site 1	85	1535	46	769	89	1263
	Site 2	88	1022	78	489	93	1034
NAQ	Site 1	80	1345	50	−344	75	465
	Site 2	82	1125	56	616	73	−10

[a] Clustering of docking poses revealed two unique binding modes. See text for more information.

[b] HINT score differences have generally been shown to relate to ΔΔG such that 515 score units ≈ −1 kcal/mol.

Table 4

Binding of ligands to site-directed mutated MORs.

Cmpd	wild type MOR (nM) ± SEM		Y210A MOR (nM) ± SEM		W318A MOR (nM) ± SEM	
	IC_{50}	K_i	IC_{50}	K_i	IC_{50}	K_i
NTX	3.90 ± 2.96	1.85 ± 1.41	0.95 ± 0.49	0.45 ± 0.23	10.35 ± 1.64	4.91 ± 0.78
NAP	2.29 ± 0.15	1.09 ± 0.07	1.61± 0.17	0.77 ± 0.08	>1000	ND[a]
NAQ	5.42 ± 0.70	2.57 ± 0.33	3.31 ± 1.71	1.57 ± 0.81	>1000	ND[a]

[a]Not determined.

Bioorg Med Chem. Author manuscript; available in PMC 2014 November 01.